

# An experimental study on FRP –concrete delamination

C. Mazzotti, B. Ferracuti & M. Savoia

*DISTART – Structural Engineering, University of Bologna, Bologna, Italy*

**ABSTRACT:** The first results of an experimental campaign on FRP – concrete delamination are presented. Four specimens with different bond lengths have been tested. Both strain gages along the FRP plate and LVDT transducers have been used. Starting from experimental data, shear stress – slips data have been computed. A non linear interface law has been calibrated. A numerical bond – slip model has been used, adopting the above mentioned law for the FRP – concrete interface. Numerical results are found to be in good agreement with experimental results.

**Keywords:** FRP, concrete, delamination, interface, experimental study

## 1 INTRODUCTION

When using FRP – plates or sheets to strengthen r.c. beams, FRP – concrete bonding is very important. Since delamination is a very brittle failure mechanism, it must be avoided in practical applications. Bonding depends on mechanical and physical properties of concrete, composite and adhesive. Definition of a correct interface law is then important to predict ultimate failure load due to delamination. It is required to estimate the effectiveness of FRP-strengthening of r.c. elements also under service loadings, due to significant stress concentrations close to transverse cracks in concrete.

Very few experimental studies can be found in literature which can be useful to calibrate a FRP – concrete interface law. Chajes et al. (1996) performed delamination tests using CFRP plates 25.4 mm wide and different bond lengths (from 50.8 mm to 203.4 mm). Taljsten (1994) conducted several delamination tests considering both steel and composite plates. Aiello & Pecce (2001) also performed several tests using FRP plates. Miller et al. (2001) adopted a particular bending set-up to perform delamination tests on carbon-fiber sheets glued to concrete. Brosens (2001) adopted a symmetric setup by gluing two CFRP sheets to two

concrete specimen subject to a traction test. In all these tests, failure load and strains along the FRP plate were measured. In Savoia et al. (2003a), experimental tests by Chajes et al. (1996) and Miller et al. (2001) were used to calibrate a non linear interface law.

In the present paper, the first results of an experimental campaign on FRP – concrete delamination are presented. Four specimens with different bonding lengths have been prepared. A number of closely spaced strain gages has been used to measure strains along the FRP plate. Moreover, LVDT transducers have been used to measure displacements. Starting from experimental data, average shear stresses between two subsequent strain gages and corresponding shear slips have been computed. These data have been used to calibrate a non linear interface law, using a two-parameter law similar to that proposed by Popovics (1973).

The (estimated) value of maximum transmissible load by an anchorage of infinite length is used to define the value of fracture energy of interface law. This quantity is used as a constraint in the calibration procedure. Fracture energy of constitutive interface law, in fact, is an important condition to be satisfied to predict the correct value of maximum transmissible load through the interface. Moreover, the softening branch, where experimen-

tal results are very scattered, is strongly influenced by the value of fracture energy.

Finally, a bond – slip model originally presented in Savoia et al. (2003b) has been used. Concrete and plates are considered as elastic materials and the proposed non linear interface law is adopted between two materials. Numerical results are found to be in good agreement with experimental results.

## 2 GEOMETRY AND MECHANICAL PROPERTIES OF SPECIMENS

In order to study the CFRP plate – concrete shear behaviour, four specimens have been realized by glueing a CFRP plate to concrete block. Four different bonded lengths have been tested: 50, 100, 200 and 400 mm.

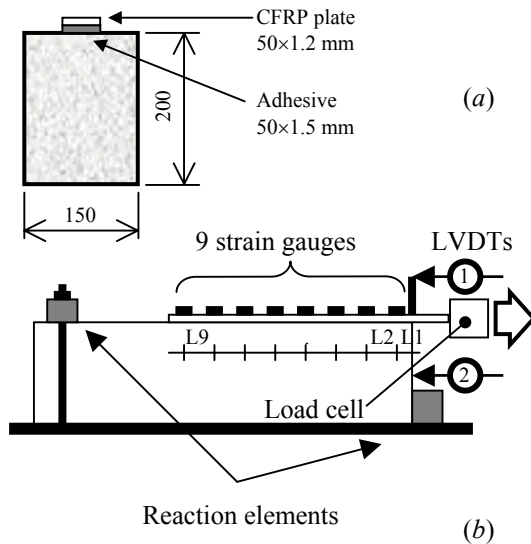


Figure 1: (a) Geometrical characteristics of FRP – concrete specimens, scheme and (b) picture of experimental setup.

Concrete blocks dimensions were 150×200×600 mm. They were fabricated using normal strength concrete. Concrete was poured into wooden forms, externally vibrated. The top was steel-troweled. Three 15 cm-diameter by 30 cm-high standard cylinders were also poured and used to evaluate mechanical properties of concrete (according to Italian standards).

Specimens were demoulded after 24 hours and covered with saturated clothes for 28 days; after that, they were stored at room temperature.

Mean compressive strength  $f_{cm} = 52.6$  MPa from compression tests and mean tensile strength  $f_{ctm} = 3.81$  MPa from indirect traction tests have been obtained on cylinders. Mean value of elastic modulus has been found  $E_{cm} = 30700$  MPa and a Poisson ratio  $\nu = 0.227$ .

For composite plates, CFRP Sika CarboDur S plates 50 mm wide and 1.2 mm thick have been used. According to technical data provided by the producer, plates have a carbon fiber volumetric content equal to 70 per cent, an epoxy matrix, a minimum tensile strength of 2200 MPa and a mean elastic modulus  $E_p = 165000$  MPa.

Top surfaces of concrete blocks have been grinded with a stone wheel to remove the top layer of mortar, just until the aggregate was visible (approximately 1 mm). Plates have been bonded to the top surface of blocks by using a 1.5 mm thickness of two – components Sikadur-30 epoxy adhesive; curing period was at least 1 day prior to testing.

## 3 THE EXPERIMENTAL SETUP

The concrete block was positioned on a rigid frame with two steel reaction elements to prevent horizontal and vertical translations (figure 1a); the free end of the plate was clamped to a steel plate that was free to rotate around the vertical axis. The traction force was applied to the steel plate by using a mechanical actuator (figure 1b); tests were performed under displacement control of the plate free end.

### 3.1 Instrumentation

A load cell has been used to record the applied traction force. Along the CFRP plate, a series of five-to-nine strain gauges (depending on the plate length) were placed, in the centreline. In Table 1, for each bonded length, spacings between strain gauges are reported, starting from the traction side of concrete block. Moreover, two LVDTs were placed in order to measure displacements (figure

1a): at the beginning of the bonded length and in the lower portion of the front side of the concrete

Table 1: Positions of strain gages along the FRP plate for the 4 specimens (in mm), depending on the bonded length (B.L.).

B.L.	L1	L2	L3	L4	L5	L6	L7	L8	L9
50	10	10	10	10					
100	10	10	20	20	10	10	10		
200	20	10	20	10	20	20	40	50	
400	20	20	30	40	40	60	60	60	60

Table 2: Levels of applied force (kN) corresponding to FRP – strain profiles in figure 2.

B.L.	F1	F2	F3	F4	F5	F6	F7	F8	F9	F10
50	1.0	2.0	3.0	4.0	5.0	6.0	7.0	7.9		
100	2.0	4.0	6.0	8.0	10.0	12.0	14.0	16.0	17.0	18.9
200	4.0	8.0	12.0	16.0	18.4					
400	4.0	8.0	12.0	16.0	20.0	20.4				

block, so that relative displacements can be computed.

## 4 RESULTS OF DELAMINATION TESTS

### 4.1 The experimental results

For the four different bonded lengths, longitudinal strains along the FRP plate at different loading levels are reported in figure 2a-d. The corresponding values of applied force are reported in Table 2. The strain at  $x=0$  corresponds to that calculated from the value of external applied force.

For bonded lengths from 100 mm to 400 mm, FRP strains are very regular for low – to – medium values of applied force, showing an exponential decay starting from the loaded section ( $x=0$ ). This strain profile corresponds to a linear behavior of the interface. For high force levels, strains tend to be almost constant along FRP plate close to loaded end, due to onset of delamination phenomenon along the bonded length; where delamination has not occurred, an exponential decay behavior can be observed again.

On the contrary, for the 50 mm bonded length, an almost linear profile of strains along the anchorage has been found, also for low levels of applied force. These profiles indicate a uniform distribution of shear stresses along the anchorage. The results clearly show that the shortest bond length is significantly smaller than the effective anchorage length (the minimum length assuring maximum FRP anchoring force).

The values of maximum transmitted forces at failure as a function of bonded length are reported in figure 3a. In all specimens, failure was caused by shearing of concrete about 1-2 mm below the

surface, together with the separation of two small symmetrical triangular concrete portions in the

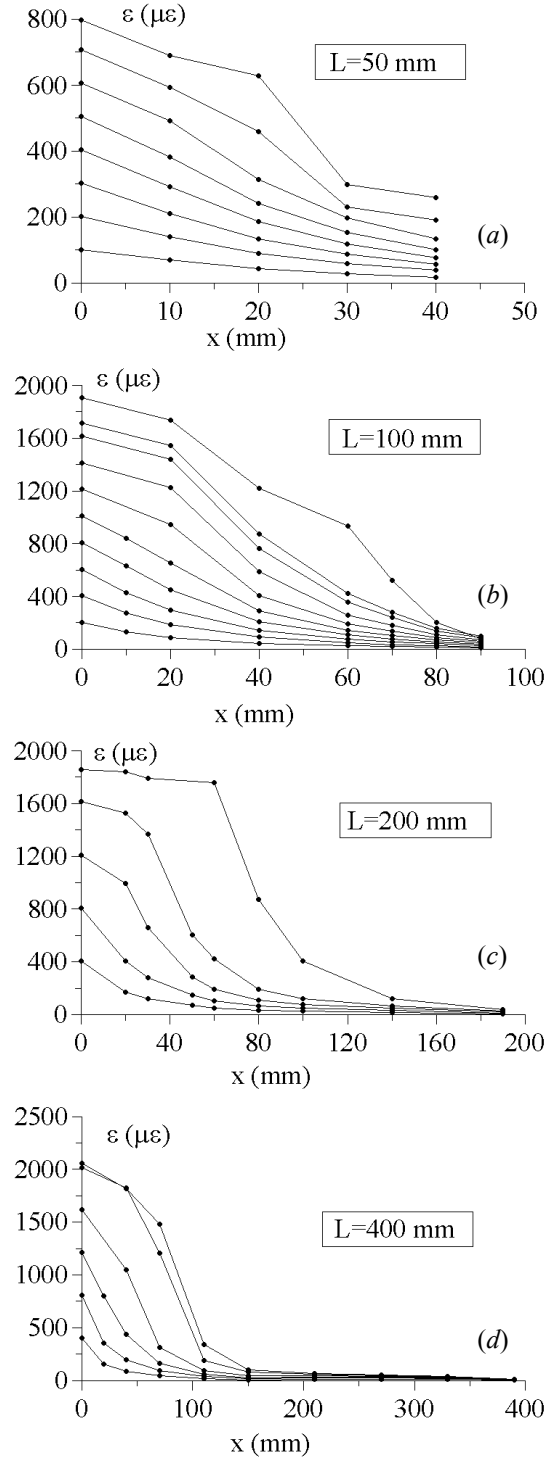


Figure 2: Profiles of experimental strains in FRP plates along the bonded lengths. Load levels are reported in Table 2.

traction side of the specimen (figure 3b). For three specimens, these portions were very similar in shape, only in the 100 mm bond length case the failure surface was larger, so explaining the high value of failure load when compared with those corresponding to 200 mm and 400 mm bonded lengths. An interpolation curve is also reported, which has been used to predict the value of maximum transmissible force by an anchorage of infinite length (see Section 5.2), for which the value  $F_{\max} = 24.44$  kN has been obtained. In the same figure, results numerically obtained using the bond – slip model described in Section 6 are also reported.

Making use of the following relation between maximum transmissible force  $F_{\max}$  and fracture energy  $G_f$  of interface law:

$$F_{\max} = b_p \sqrt{2E_p h_p G_f}, \quad (1)$$

where  $E_p$ ,  $h_p$ ,  $b_p$  are elastic modulus, thickness and width of the plate, respectively, the value  $G_f = 0.60$  N/mm has been obtained.

Eqn (1) has been derived by Ferrari (2003) and reported in Savoia et al. (2003b) with reference to a general non linear interface law. Eqn (1) was

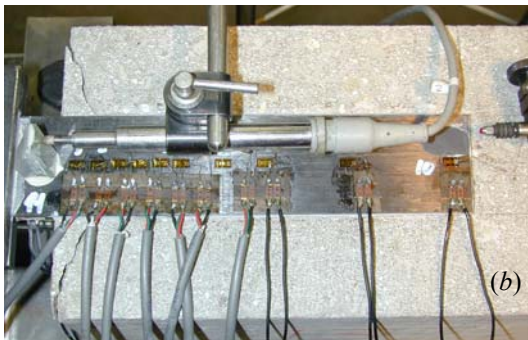
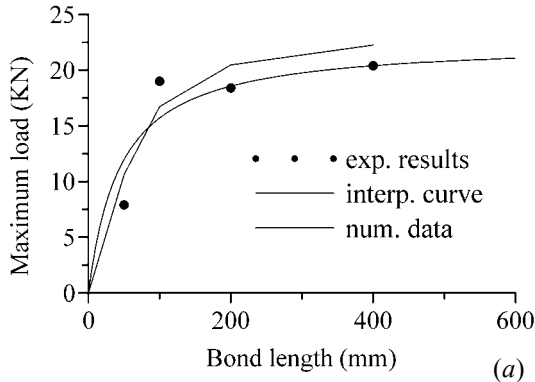


Figure 3: (a) Delamination loads as a function of bond length: experimental results and numerical simulation; (b) Picture of specimen after delamination.

previously derived by Wu et al. (2002) for a bilinear interface law and by Brosens (2001) in the case of a power law.

According to *fib* (2001), fracture energy of interface law is given by the formula:

$$G_f = 0.5 \cdot 0.23^2 \sqrt{f_{ck} f_{ctm}} = 0.345 \text{ kN/mm},$$

where concrete failure is assumed. Hence, in the present case *fib* (2001) provisions underestimate fracture energy by 45 percent.

Moreover, according to Neubauer & Rostasy (1997), maximum transmissible force and maximum anchorage length are in the present case equal to:

$$F_{\max} = 0.64 k_b b \sqrt{E_p h_p f_{ctm}} = 21.51 \text{ kN},$$

$$l_{b,\max} = 1.44 \sqrt{\frac{E_p h_p}{\sqrt{f_{ctm}} \cdot f_{ck}}} = 177.51 \text{ mm}, \quad (2)$$

where  $b$  is the concrete width. In eqn (2), coefficient  $k_b$  is a geometric factor taking into account the size effect and the different widths of concrete and plate. In the present case,  $k_b = 1.29$ .

Finally, figures 4a-b show the applied load - displacement curves for bonded lengths equal to 200 mm and 400 mm. Relative displacement  $u$  has been evaluated as the difference between displacement of loaded extremity of the plate (LVDT-1) and that of reaction support (LVDT-2). In both cases, displacement at peak load is about 0.2 mm.

#### 4.2 Post-processing of experimental results

Values of FRP strains along the plate have been used to calculate the shear stress and slip distributions along the bonded lengths. Considering an elastic behavior for the composite, the average value of shear stress between two subsequent strain gauges can be written as a function of the difference of measured strains as:

$$\bar{\tau}_{i+1/2} = \frac{E_p A_p (\varepsilon_{i+1} - \varepsilon_i)}{b_p (x_{i+1} - x_i)}, \quad (3)$$

with  $A_p$  being cross section of the composite. Moreover,  $x_i$  denotes the strain gauge position and  $\varepsilon_i$  the measured strain.

Assuming, for the sake of simplicity, perfect bonding at last strain gauge position (no slip) and neglecting concrete strain with respect to FRP counterpart, integration of strain profile gives the

following expression for the slip at  $x$ , with  $x_i \leq x \leq x_{i+1}$ :

$$s(x) = s(x_i) + \int_0^x \varepsilon(x) dx = s(x_i) + \frac{(\varepsilon_{i+1} - \varepsilon_i) x^2}{(x_{i+1} - x_i) 2} + \varepsilon_i x \quad (4)$$

When computing shear stresses and slips, some irregular values in FRP strain profiles for high loadings have been removed. For the four bonded lengths, the so-obtained shear stress-slip couples ( $\bar{\tau}_{i+1/2}$ ,  $\bar{s}_{i+1/2}$ ), at loading levels reported in Table 2, are shown in figure 5.

Comparing the data, some interesting conclusions can be drawn:

a) Stiffness of initial branch (slip  $\leq 0.02$  mm) is almost independent of bond length and loading level. The only exception is represented by the results from the smallest bond length case (50 mm). In this case, the length is so small that the actual slip never vanishes along the interface. Hence, the procedure adopted to obtain slips along the plate (see eqn (4)) underestimates the actual slip. For this reason, these data have not been used to calibrate the interface law (see section 5.2).

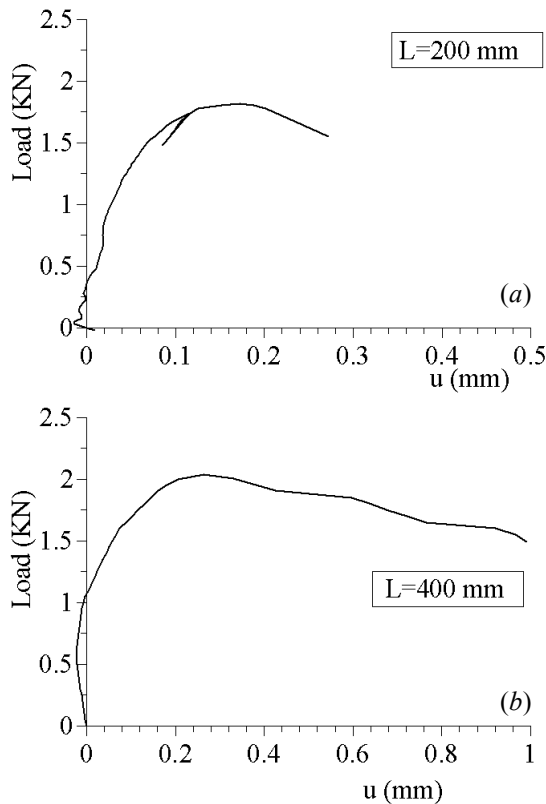


Figure 4: Load – displacement curves for bonded lengths  $BL = (a)$  200 mm and  $(b)$  400 mm.

b) Data sets exhibit a maximum value of shear stress corresponding to a slips of about 0.03-0.04 mm; for higher slips, an evident softening behavior

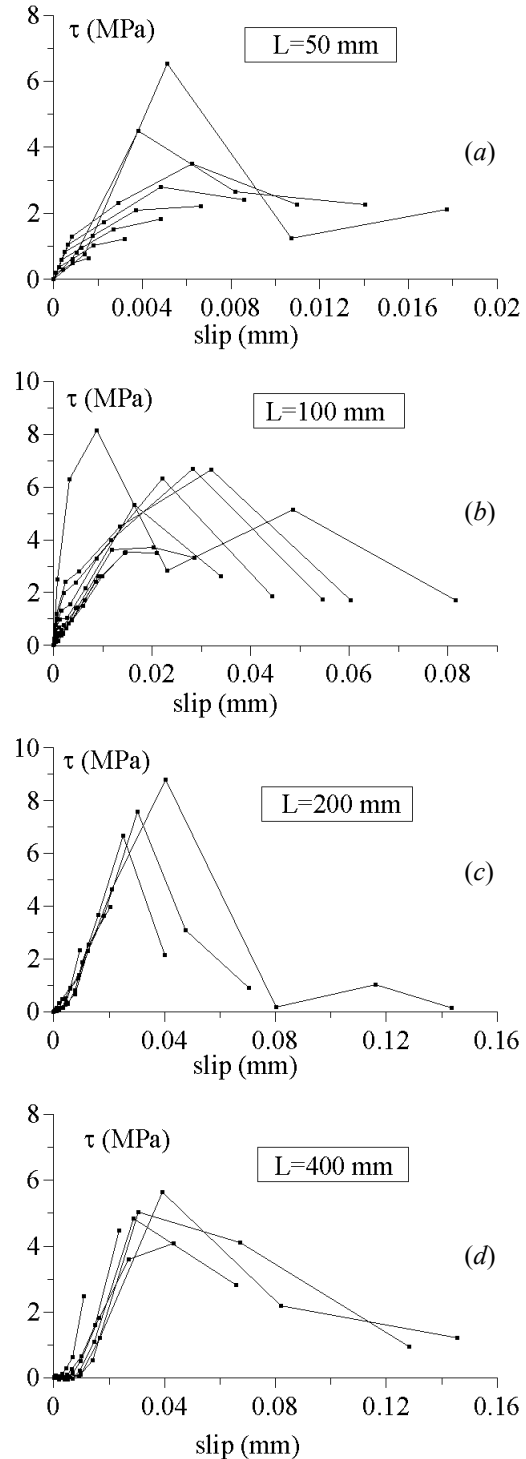


Figure 5: Average shear stress – slip data obtained from post-processing experimental results.

has been found, with shear stress decreasing for increasing values of FRP-concrete slip. Experimental results are in this region very scattered.

## 5 CALIBRATION OF A NON LINEAR INTERFACE LAW

### 5.1 The interface law

The interface law must reproduce an almost linearly elastic behavior for small slips, a maximum value for shear stress and a softening branch for higher slips.

In the present study, a fractional law is adopted:

$$\tau_p = \bar{\tau} \frac{s_p}{\bar{s}} \frac{n}{(n-1) + (s_p/\bar{s})^n}, \quad (5)$$

similar to that adopted by Popovics (1973) for constitutive law of concrete under compression.

In eqn (5),  $(\bar{\tau}, \bar{s})$  indicates the maximum shear stress and the corresponding slip, whereas  $n > 2$  is a parameter mainly governing the softening branch.

The fracture energy of the law can be analytically obtained in the form:

$$G_f = \int_0^{+\infty} \tau_p(s_p) ds_p = g_f(n) \bar{\tau} \bar{s}, \quad (6)$$

where  $g_f$  is given by:

$$g_f(n) = \pi \left( \frac{1}{n-1} \right)^{1-\frac{2}{n}} \frac{1}{\sin(2\pi/n)}. \quad (7)$$

It can be verified that  $g_f \rightarrow 1/2$  for  $n \rightarrow \infty$ , condition corresponding to elastic-brittle behavior. Moreover, eqn (7) confirms that Popovics equation (5) requires  $n > 2$ ; otherwise, the fracture energy might not be a positive and finite quantity.

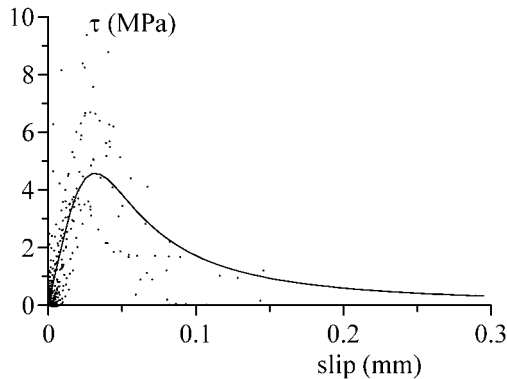


Figure 6: The proposed non linear interface law and data obtained from post-processing experimental results.

### 5.2 Calibration of the law

Both shear stress – strain data  $(\bar{\tau}_{i+1/2}, \bar{s}_{i+1/2})$  and fracture energy  $G_f$  are used to evaluate the three unknown parameters of interface law in eqn (5), i.e.,  $\bar{\tau}, \bar{s}, n$ .

A least square minimization between theoretical and experimental shear stress – strain data is performed, adopting as a constraint in the minimization procedure the value of fracture energy obtained from eqn (1), i.e.,

$$\min_{\bar{\tau}, \bar{s}, n} \sum_{i=1}^m (\tau_i(\bar{\tau}, \bar{s}, n) - \tau_{\text{exp},i})^2$$

subject to  $G_f = g_f(n) \bar{\tau} \bar{s} = \frac{F_{\text{max,exp}}^2}{2 E_p h_p b_p^2}, \quad (8)$

where  $m$  is the number of experimental data.

This procedure is very simple, since, from eqn (8b), the peak slip  $\bar{s}$  can be written as an explicit function of the remaining parameters  $\bar{\tau}, n$ ; the optimization procedure is then a two-parameter minimization.

The values  $\bar{\tau} = 4.58$  MPa,  $\bar{s} = 0.03$  mm,  $n = 2.61$  have been obtained. In figure 6 the proposed interface law is reported, together with all shear stress – slip experimental data. It is worth noting that the proposed law is in good agreement with experimental data for slips smaller than  $\bar{s}$ , corresponding to maximum shear stress; for higher slips, the experimental results are very scattered.

*Fib* (2001) provisions predict, for the present case, the maximum bond stress as:

$$\tau_{\text{max}} = 0.285 k_b \sqrt{f_{ck} f_{ctm}} = 3.71 \text{ MPa}. \quad (9)$$

## 6 NUMERICAL SIMULATIONS OF TESTS

Experimental tests have been numerically simulated, in order to verify the accuracy of the proposed plate – concrete interface law.

A bond-slip kinematic model has been adopted, originally presented in Savoia et al. (2003b), to which the reader is addressed for additional details. The model is based on the assumption of pure extension for two different materials, concrete and FRP plate (no bending). Linear elasticity is adopted for concrete and plate, whereas the non linear law (5) is used for the interface between two materials. Then, a Finite Difference discretization is used for the unknown variables (axial displacements and stress resultants of concrete and plate).

Comparison between experimental and numerical results are reported in figures 3 and 7–8.

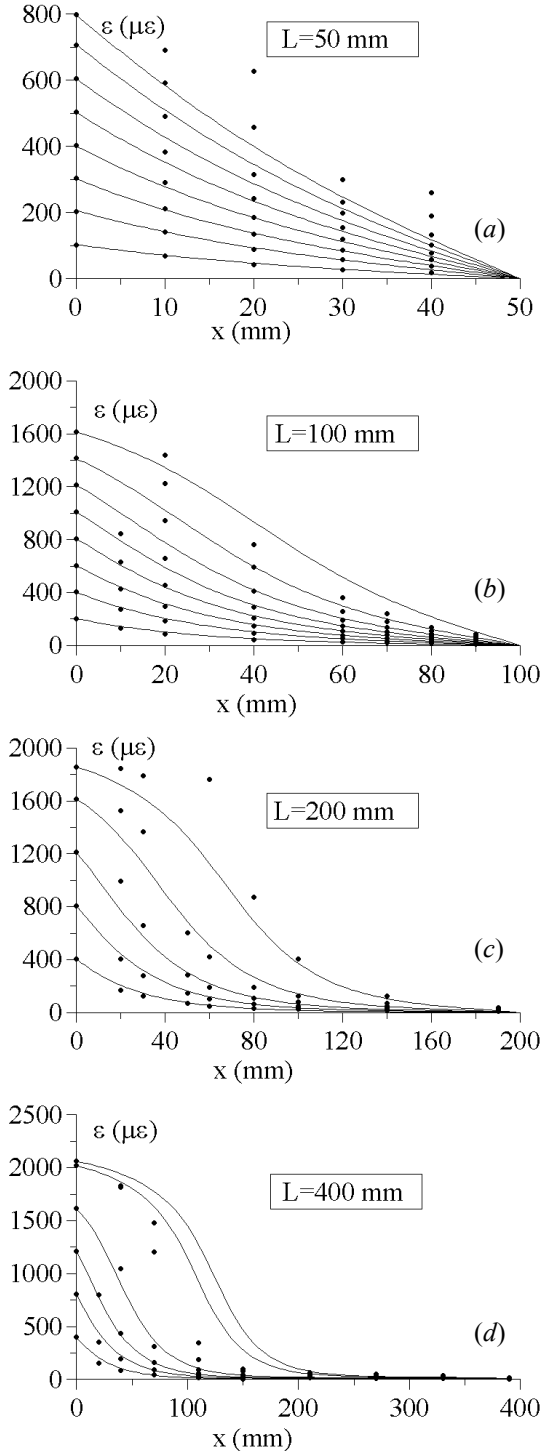


Figure 7: Profiles of strains along FRP plate: comparison between numerical and experimental results.

In figure 3, delamination failure load obtained numerically as a function of bonded length is compared with experimental results. The results confirm that the proposed interface law provides for a good prediction of failure loads also for small bonding lengths.

Strain distributions in FRP plate along the bonded length are reported in figure 7a-d for the four different cases. The higher load level is close to failure load obtained experimentally.

Numerical results are generally in very good agreement with experimental data (considering the unavoidable scattering of experimental results at higher load level). For all bonded lengths, the behavior for low load levels is very well predicted, so assuring that stiffness of initial (elastic) branch of interface law is correctly evaluated.

Shear stress distributions for bonded lengths equal to 100 mm and 400 mm are reported in figure 8. Very good agreement between numerical and experimental results is generally found for low – to – medium loadings. For very high loads, i.e., close to plate delamination, results obtained from experimental data are more irregular. In any case, the maximum value of shear stress and, often, also its position and the gradient of shear stress distribution along the bonded length are well predicted.

## 7 CONCLUSIONS

Results from a set of experimental delamination tests have been presented. Applied force, displacements and strains along FRP plate have been measured. Values of applied force have been used to estimate the fracture energy of interface law. The obtained results are compared with expressions reported in *fib* (2001).

An interface shear stress – slip law has then been calibrated starting from experimental data, adopting the value of fracture energy as a constraint in the minimization procedure between experimental and predicted values. Finally, numerical simulations have also been performed. Results are found to be in good agreement with experimental results.

These results represent the first step of an experimental campaign on FRP – concrete delamination, where different plate widths will be tested. It is well recognized that maximum shear stress (evaluated in the form of eqn (3)) increases when plate width decreases.

The final aim is to develop rules for defining an FRP – concrete interface law as a function of

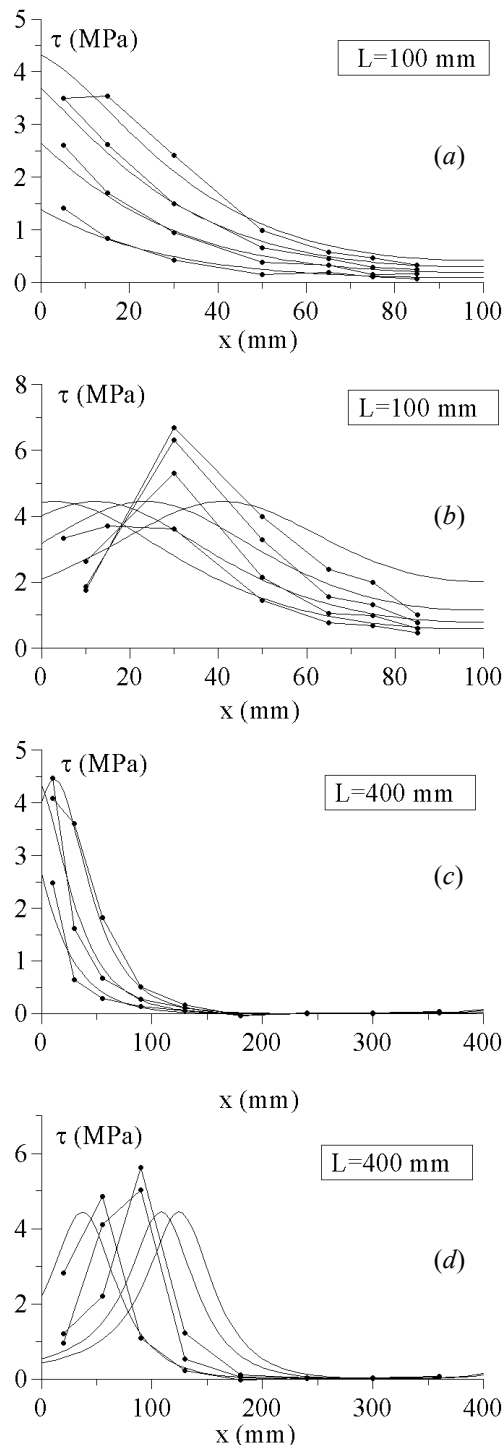


Figure 8: Profiles of shear stresses along FRP plate for 100 and 400 mm bonded length. Comparison between numerical and experimental results: a), c) low and b), d) high loading levels.

constituents (FRP plates and concrete material and geometrical properties).

## ACKNOWLEDGEMENTS

The authors would like to thank the Sika Italia S.p.A. for providing CFRP plates and adhesives for the specimens. The financial supports of (italian) MIUR (PRIN 2001 and PRIN 2003 Grants, FIRB Grant) and C.N.R., PAAS Grant 2001 are gratefully acknowledged.

## REFERENCES

- Aiello, M.A. & Pecce M. 2001. Experimental bond behavior between FRP sheets and concrete. In *Structural faults and repair Conference; Proc. intern. symp.*, London. 4-6 July 2001.
- Brosens K. 2001. *Anchorage of externally bonded steel plates and CFRP laminates for the strengthening of concrete elements* (doctoral thesis). University of Leuven, Belgium.
- Chajes M.J., Finch W.W. jr, Januska T.F. & Thomson T.A. jr. 1996. Bond and force transfer of composite material plates bonded to concrete. *ACI Structural J.* Vol. 93: 208-217.
- Ferrari (2003). Private communication.
- Fib 2001. *Externally bonded FRP reinforcement for RC structures*. Technical report, Bulletin n° 14.
- Miller B., Nanni A. & De Lorenzis L. 2001. Bond of FRP laminates to concrete. *ACI Material J.* Vol. 98(3): 246-254.
- Neubauer U. & Rostasy F. S. 1997. Design aspects of concrete structures strengthened with externally bonded CFRP – plates. In *Concrete+composites, Proc. of 7th Int. Conf. on Struct. Faults & Repairs* Vol. 2: 109-118.
- Popovics S. 1973. A numerical approach to the complete stress-strain relation for concrete. *Cem. Conc. Res.* Vol. 3(5): 583-599.
- Savoia, M., Ferracuti B. & Mazzotti C. 2003a. Delamination of FRP plate/sheets used for strengthening of R/C elements. In Franco Bontempi (ed.), *System-based vision for strategic and creative design; Proc. intern. symp., Rome 23-26 September 2003*. Rotterdam: Balkema, Vol. 2: 1375-1361.
- Savoia M., Ferracuti B. & Mazzotti C. 2003b. Non linear bond-slip law for FRP-concrete interface. In *FRPRCS-6; Proc. intern. symp.*, Singapore, July 2003.
- Täljsten B. 1994. *Plate bonding* (doctoral thesis). Division of Structural Engineering, Luleå University, Sweden.
- Wu Z., Yuan H. & Niu H. 2002. Stress transfer and fracture propagation in different kinds of adhesive joints. *J. Eng. Mech. ASCE* Vol. 128(5): 562-573.